

## **Computational analysis of congenital heart disease associated SNPs: Unveiling their impact on the gene regulatory system**

### **Authors**

Shikha Vashisht<sup>1</sup>, Costantino Parisi<sup>1</sup>, Cecilia L. Winata<sup>1\*</sup>

### **Affiliations**

<sup>1</sup> International Institute of Molecular and Cell Biology in Warsaw, Laboratory of Zebrafish Developmental Genomics, Księcia Trojdena 4, 02-109, Warsaw, Poland

**\*Corresponding Author**

## Abstract

Congenital heart disease (CHD) is a prevalent condition characterized by defective heart development, causing premature death and stillbirths among infants. Genome-wide association studies (GWASs) have provided insights into the role of genetic variants in CHD pathogenesis through the identification of a comprehensive set of single-nucleotide polymorphisms (SNPs). Notably, 90-95% of these variants reside in the noncoding genome, complicating the understanding of their underlying mechanisms. Here, we developed a systematic computational pipeline for the identification and analysis of CHD-associated SNPs spanning both coding and noncoding regions of the genome. Initially, we curated a thorough dataset of SNPs from GWAS-catalog and ClinVar database and filtered them based on CHD-related traits. Subsequently, these CHD-SNPs were annotated and categorized into noncoding and coding regions based on their location. To study the functional implications of noncoding CHD-SNPs, we cross-validated them with enhancer-specific histone modification marks from developing human heart across 9 Carnegie stages and identified potential cardiac enhancers. This approach led to the identification of 2,056 CHD-associated putative enhancers (CHD-enhancers), 38.9% of them overlapping with known enhancers catalogued in human enhancer disease database. We identified heart-related transcription factor binding sites within these CHD-enhancers, offering insights into the impact of SNPs on TF binding. Conservation analysis further revealed that many of these CHD-enhancers were highly conserved across vertebrates, suggesting their evolutionary significance. Utilizing heart-specific expression quantitative trait loci data, we further identified a subset of 63 CHD-SNPs with regulatory potential distributed across various cardiac tissues. Concurrently, coding CHD-SNPs were represented as a protein interaction network and its subsequent binding energy analysis focused on a pair of proteins within this network, pinpointed a deleterious coding CHD-SNP, *rs770030288*, located in C2 domain of *MYBPC3* protein. Overall, our findings demonstrate that SNPs have the potential to disrupt gene regulatory systems, either by affecting enhancer sequences or modulating protein-protein interactions, which can lead to abnormal developmental processes contributing to CHD pathogenesis.

**Keywords:** Congenital heart disease, Single-nucleotide polymorphisms, Enhancer, Protein-Protein Interaction Network, Gene regulatory system

## Authors Summary

Congenital heart disease (CHD) is a common condition with defects in heart development present from birth. CHD symptoms can range from mild to severe, often requiring early intervention or surgery. Over the years, numerous research studies have indicated the association of single nucleotide polymorphisms (SNPs) with CHD. However, the challenge arises from the fact that the majority of these variants are located within the noncoding portion of the genome, making it difficult to comprehend their mechanism of action. Here, we present a systematic computational pipeline to identify SNPs associated with CHD, in both protein-coding and noncoding regulatory elements – specifically, enhancers. Utilizing this pipeline, we established a collection of putative enhancers containing CHD-SNPs. Within these enhancers, several transcription factor binding sites (TFBSs) related to heart developmental processes were identified. The presence of SNPs in these sites may potentially impact the binding of TFs necessary for the expression of genes targeted by these enhancers. Additionally, some of these enhancers were also found to be evolutionary conserved, suggesting their functional relevance. Concurrently, we identified coding variants which can alter the protein-protein interactions in a protein interaction network. Taken together, our study provided critical insights into the role of genetic variants in the pathological mechanism of complex human diseases, including CHD.

## Introduction

Congenital heart disease (CHD) is a defect of the heart caused by abnormalities in the process of its development. It is one of the most common birth defects characterized by a wide range of structural deformities of the heart and great vessels, affecting 10 per 1000 (~1%) neonates worldwide, along with 10% of stillbirths (1–4). The complex multifactorial etiology of CHD presents a major challenge towards understanding its clear pathological mechanism. A large number of protein-coding genes are known to be implicated in CHD (5–7). However, whole genome sequencing (WGS) data from thousands of CHD patients and genome-wide association studies (GWAS), have revealed that the majority (~95%) of CHD-causing genetic variants fall within the noncoding fraction of the genome (8,9). Despite tremendous progress made towards their identification, we still lack clarity on how noncoding genetic variants associated with CHD-traits are implicated in defective heart formation (10). Hence, there is a fundamental need to discover the contribution of noncoding variants towards CHD development and its manifestation to offer novel insights into the genetic basis of CHD.

Noncoding genetic variants could alter normal developmental processes by disrupting the function of enhancers (11). It is estimated that the number of disease-associated variants impacting enhancer function far exceeds that affecting protein-coding genes (12,13). Enhancers are a major type of *cis*-regulatory element in the genome which regulates the expression of downstream target genes. They serve as binding sites for transcription factors (TFs) which are necessary for the activation of target gene expression. Genetic variants within enhancers could therefore disrupt TF binding sites (TFBSs), causing the failure of TF binding and ultimately loss of enhancer function associated with disease (14,15). Despite the wealth of data available on putative enhancers, there is still a lack of systematic analyses focused on particular biological context within development and disease. Moreover, validating the enhancer activity of these millions of regions, as well as ascribing their function and target genes still poses an uphill task. Further, the ability to link enhancers to their putative target genes could provide additional critical insights into their possible role in specific biological processes, particularly if the function of the target is already known. A comprehensive map of genetic interactions consisting of not only protein coding genes, but also enhancers regulating their expression, could therefore contribute valuable insight into their function and mechanism in regulating specific biological processes.

In this study, we present a catalogue of 2,056 putative human cardiac enhancers and a protein-protein interaction network associated with CHD through a systematic compilation and analyses of CHD-specific GWAS data. To achieve this, we devised a computational pipeline to process SNPs spanning both noncoding and coding regions of the genome. Using noncoding CHD-SNPs data, we predicted CHD-enhancers through a rational integration of epigenomics data of human heart organogenesis followed by conservation analyses and intersection with expression quantitative trait loci (eQTL) data to establish their regulatory potential. The identified set of cardiac enhancers contained specific TF binding sites specifically linked to heart function which further support their functional relevance.

Parallel investigation into coding CHD-SNPs focused on their potential impact on protein-protein interaction stability, we first constructed a protein-protein interaction network (PPIN, **Fig S1**) and analyzed the interaction between two crucial cardiac sarcomeric proteins—cardiac myosin binding protein-C (*MYBPC3*) and cardiac  $\alpha$ -actin (*ACTC1*) (16). Prior studies revealed a substantial number of individuals with hypertrophic cardiomyopathy (HCM) and dilated cardiomyopathy exhibit alterations in sarcomeric proteins (17,18). Examining changes in binding energy within the three-dimensional structures of these proteins revealed a deleterious

missense SNP (c.1256G>A; p.Arg419His; *rs770030288*). This mutation exhibited a notably higher potential to destabilize the interaction between these proteins, emphasizing the significance of this mutation in the context of protein stability and cardiac function. Taken together, these results highlight the potential significance of our approach in contributing to the understanding of genetic factors influencing CHD, providing a holistic perspective on both regulatory and coding elements.

## RESULTS

### 1. A compilation of CHD-associated single nucleotide polymorphisms and their annotations

To identify CHD-associated SNPs, we retrieved data from single nucleotide polymorphism (SNP) resources based on Genome-wide Association Studies (GWAS), including NHGRI-EBI GWAS-catalog (19) and ClinVar (20,21) databases. This systematic approach resulted in a cumulative set of 15,876 CHD-SNPs (computational pipeline illustrated in **Fig 1A**). As of August, 2023, the GWAS-Catalog contains a total of 5,39,949 SNPs while ClinVar database consists of a total of 4,609,367 variations including SNPs and other types of genomic variations. In GWAS-catalog, out of 5,39,949 SNPs, 1,884 unique statistically significant ( $p$ -value  $< 10e-6$ ) SNPs were found to be associated with CHD-related traits (4,22–25) (CHD-SNPs; **Table S1 and S2**). Consequently, ClinVar consisted of 4,609,367 variations, out of which we retrieved 15,248 unique CHD-specific variations which consisted of 13,992 CHD-SNPs and other types of variations, including 629 deletions, 287 duplications, 107 indels, 43 insertions and 190 microsatellites (**Table S3**). Further, ANNOVAR (26) annotation of CHD-related variants revealed that, from GWAS-catalog, 33.55 % and 43.63% lies within the intergenic and intronic regions of the genome while only 4.46% of the variants were from the exonic part of the genome (**Fig 1B**). On contrary, ClinVar database consisted of a large percentage (83.54%) of CHD-SNPs within the exonic part of the genome while only 0.01% and 7.03% of the CHD-SNPs were present on intergenic and intronic regions, respectively (**Fig 1C**). These differences exist mainly due to the fact that more than 80% of ClinVar associations result from whole exome sequencing studies (WES), thus predominantly capturing the protein-coding part of the genome. Additionally, ClinVar primarily deposits fully curated and clinically tested genetic variations.

Based on their location, CHD-SNPs were classified into: (i) coding, indicative of sequences that transcribe into proteins, and (ii) noncoding, denoting sequences void of protein-coding potential. Noncoding regions specifically encompass distal intergenic, intronic, and promoter regions, the latter of which is demarcated by the stretch of region from 1kb upstream to 1kb downstream of the transcription start site (TSS). In total, out of 1,884 CHD-SNPs extracted from the GWAS-catalog, 163 and 1,721 were located in coding and noncoding regions of the genome, respectively. The latter consisted of 632 in distal intergenic, 822 in intronic, 216 in ncRNA-intronic and 51 in promoter regions. While in the ClinVar database, out of 13,392 CHD-SNPs, we obtained 12,171 within coding and 1,221 within noncoding genomic regions, with the latter consisting of 2 in distal intergenic, 984 in intronic, 214 in ncRNA-intronic and 21 in promoter regions.

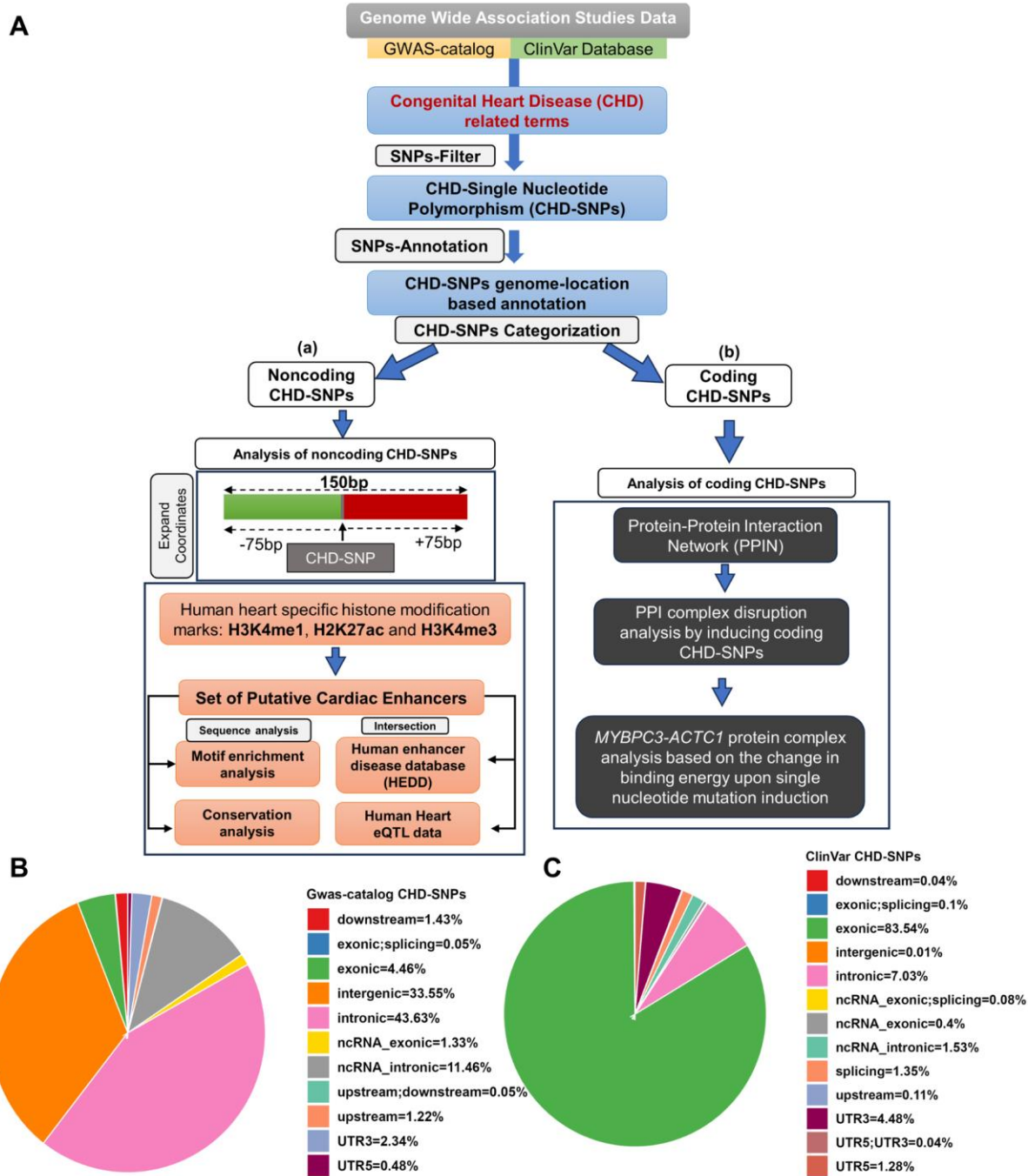


**Fig 1:** A computational workflow detailing the extraction of variant-trait data from genome-wide association studies, their filtration using congenital heart disease (CHD) associated terms and annotation using ANNOVAR. Post-filtration and annotation, CHD-SNPs undergo two-way analysis, depicted as (a) Analysis of noncoding CHD-SNPs and (b) Analysis of coding CHD-SNPs in the workflow. **B, C** Pie Charts illustrating the genomic distribution of CHD-SNPs obtained from GWAS-catalog and ClinVar database.

## 2. Identification of a potential set of human cardiac enhancers

We then sought to ascertain the identity of the noncoding CHD-SNP containing regions as enhancers. Enhancer regions are enriched by specific histone modification marks which could also indicate their activity (27–30). Among these histone modification marks, H3K4me1 is



associated with the presence of enhancers, while the presence of H3K27ac is a signature of active enhancers, differentiating them from their poised counterparts (31). Additionally, H3K4me3 predominantly marks promoter sequences (32,33). We hypothesize that noncoding CHD-SNPs might disrupt enhancer regions and consequently, TF binding. To test this, we first sought to assess the region carrying the CHD-SNP as functional enhancers. For this purpose, each noncoding CHD-SNP was expanded by 75bp on both flanks, yielding a 150bp genomic segment with the SNP centrally located. We then probed these segments for the presence of enhancer-specific histone modification marks. Utilizing epigenomic datasets (34) from human heart organogenesis across nine Carnegie stages (CS13, CS14, CS16-21, CS23), we sought regions marked by histone modification marks H3K4me1, H3K27ac, and H3K4me3 ( $pvalueSignal \geq 9.0$ ). Such elements exhibiting significant enrichment for these marks were designated as putative cardiac enhancers. Together, we obtained a set of 2,056 CHD-SNP-containing putative cardiac enhancers (CHD-enhancers) (**Table S4**), which consisted of 1,139 from GWAS-catalog and 917 from the ClinVar database. The analysis of CHD-enhancers distribution across Carnegie stages, illustrated in **Fig 2A**, unveils the dynamic landscape of CHD-enhancers shaping the embryonic development of the heart. Notably, the highest count of 1,138 enhancers identified in the later developmental stage (CS23) while in the initial stage (CS13) 821 enhancers were predicted. The lowest number of enhancers, 97, were observed in CS17. Moreover, the co-occurrence of the predicted enhancers was also predicted, as shown in the intersection set in **Fig 2A**, where, for instance, out of the 821 identified enhancers in CS13, 530 were found to be expressed in other stages too, while 291 were specific to CS13. Furthermore, the occurrence of each predicted CHD-enhancer in a specific developmental stage, its presence in other stages, or its absence, revealed intricate patterns of regulatory activity throughout embryonic heart development (**Fig 2B**).

Subsequently, to corroborate our findings, we cross-referenced CHD-enhancers with human enhancer disease database (HEDD) (35). This intersection resulted in the identification of 801 enhancers that overlapped with CHD-enhancers (**Table S5**). Further, we categorized CHD-enhancers based on their *macs2pval* signal across all Carnegie stages. This resulted in 55 early, 85 intermediate, 205 late, 2 early-late and 17 always-active putative cardiac enhancers (**Fig 2C; Table S6**).

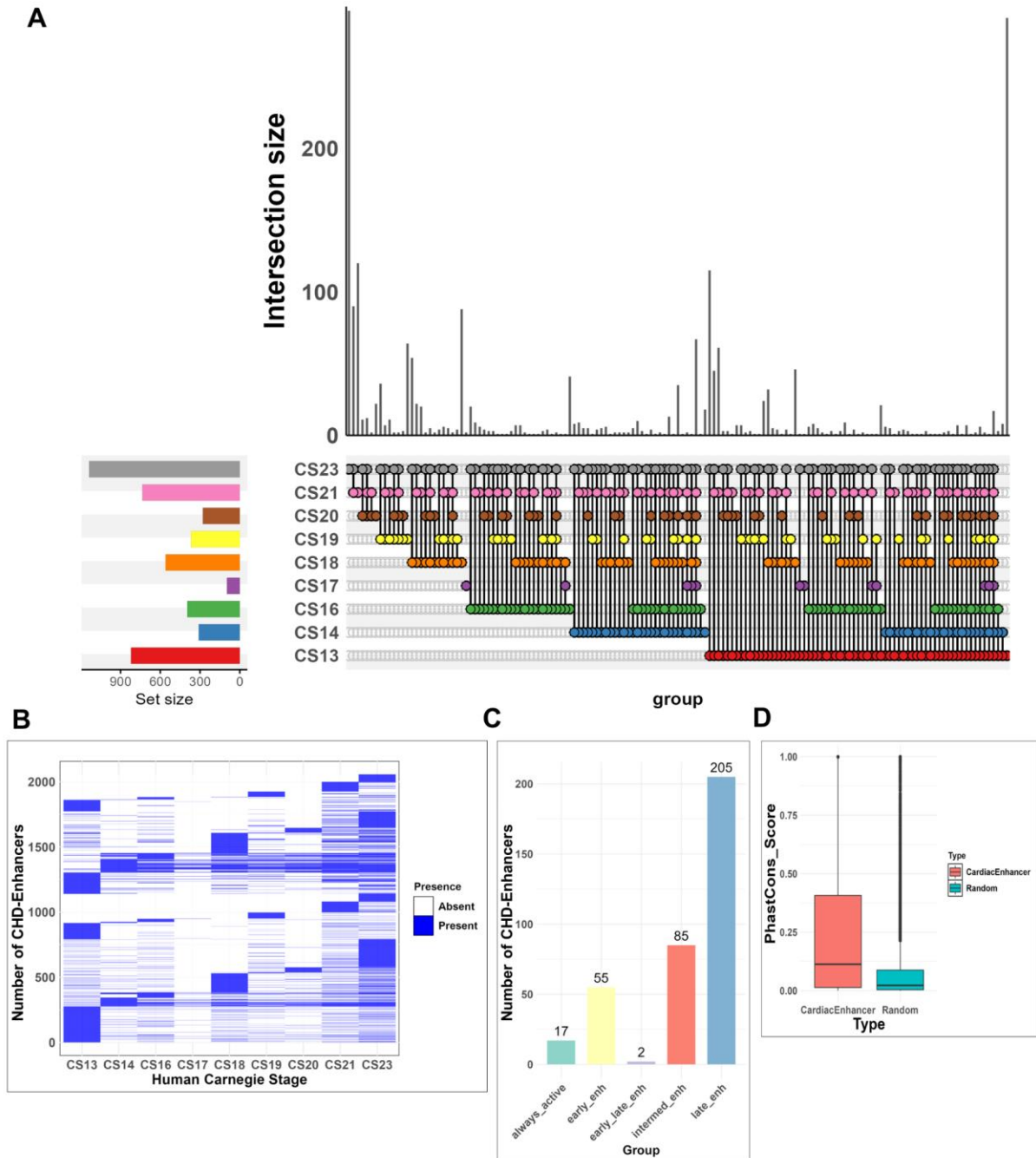


**Fig 2: A.** An upset plot showing the distribution and intersections of putative cardiac enhancers across nine Carnegie stages (CS13, CS14, CS15, CS16-21, CS23). Each vertical bar (shown in ‘dark grey’ color) indicates the number of occurrences of enhancers for an individual and combination of stages, while horizontal bars at the bottom denote the total enhancer counts for each stage. **B.** A heatmap representing the distribution of CHD-enhancers identified across nine distinct Carnegie stages (CS13, CS14, CS15, CS16-21, CS23). The color gradient ranging from ‘white’ to ‘blue’ signifies the degree of enhancer-specific histone modification signals, where ‘blue’ marks the presence of a significant enhancer signal in a given stage and ‘white’ indicates no detectable signal. **C.** A bar chart represents the stage-wise distribution of CHD-enhancers selected based on their presence in minimum 5 or more Carnegie stages. The categories include: (i) *always\_active* enhancers: These show consistent activity across all Carnegie stages due to the presence of enhancer-specific histone modification marks. (ii) *early\_enh*: represents enhancers active during Carnegie stages CS13,14,16. (iii) *intermed\_enh*: active during stages

CS17-19. (iv) *late\_enh*: active during stages CS20,21,23. (v) *early\_late\_enh*: exhibits activity during both early and late Carnegie stages. **D.** A boxplot showing the comparison between conservation scores of putative cardiac enhancers (represented in 'salmon' colored box) and random noncoding genomic sequences (depicted in 'turquoise').

### 3. Enrichment of transcription factor binding motifs in putative cardiac enhancer regions

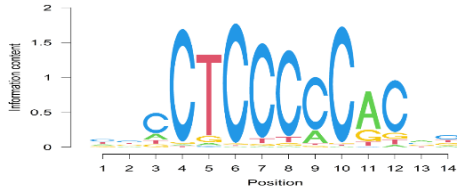
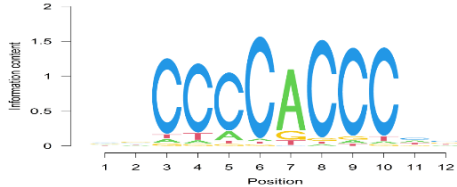
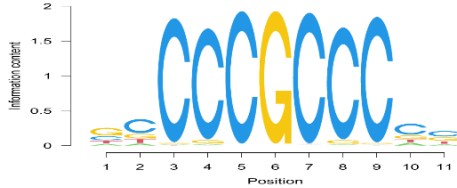
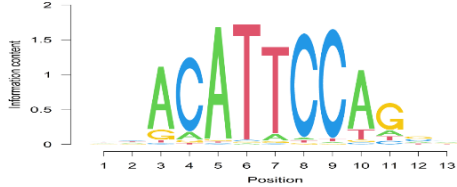
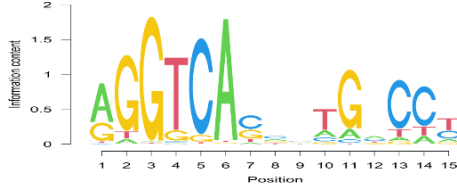
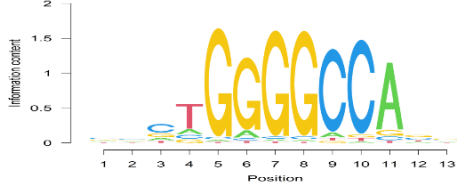
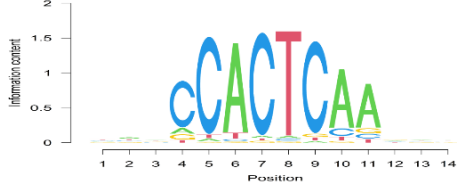
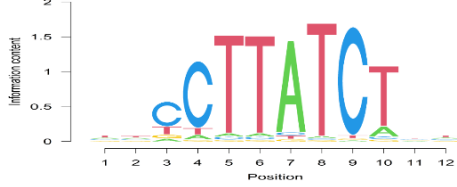
Enhancers regulate gene activity by binding to tissue-specific TFs at specific sites known as transcription factor binding sites or motifs (TFBSs) (36,37). Disease-associated noncoding variants within enhancer regions often perturb the TFBSs, resulting in disrupted transcriptional output of their target genes (38). To prioritize CHD-enhancers based on their potential regulatory function and study CHD-specific regulatory networks, CHD-enhancer regions were analyzed for the presence of TFBSs. From the motif enrichment analysis, we identified 163 statistically significant TFBSs (threshold on q-value < 0.05) (**Table S7**). Notably, many of these identified TFs play specific roles in early cardiac development, valvulogenesis, and cardiac maturation processes (**Table 1**). Among the TFBSs identified was that of Wilms' tumor-1 (*Wt1*) (q-value=0.00023), known for its expression in cardiac endothelial cells during both normal heart development and post-infarction periods (39). Prior studies have elucidated its vital role in heart vessel formation (39). Another TF identified in this analysis was GATA Binding Protein 4 (*GATA4*) which is known to play a pivotal role in cardiac progenitor cells specification and cardiac septation (40). Additionally, our analysis revealed a significant over-representation of TFBSs from the Kruppel-like factor (*KLF*) family, recognized for their specialized roles in heart development (41). These included *KLF2* (42,43), *KLF4* (44,45), and *KLF15* (46), the latter shown to be overexpressed during episodes of heart pressure overload, typically seen in hypertrophic cardiomyopathies. It also regulates *GATA4* expression to stabilize cardiomyocyte size (46). Our analysis also identified the TFBS for Spleen focus forming virus proviral integration oncogene (*SPI1*), known for its heightened expression post-myocardial infarction (47). From the TEAD TF family, *TEAD1* was enriched, documented for its expression in adult mammalian hearts and association with normal heart contractility where its mutations can lead to dilated cardiomyopathy (48).

Other significant TFBSs enriched among the CHD-enhancers include Estrogen Related Receptor Alpha (*ESRRA*), known for its pivotal role in postnatal cardiac maturation through mitochondria-focused biogenesis in cardiomyocytes (49); PLAG1 Like Zinc Finger 1 (*PLAGL1*), important for sarcomere development and contractility in cardiomyocytes (50,51); and TGFB induced factor homeobox 1 (*TGIF1*), with an established role in a cardiac neural crest pathway crucial for the proper septation of the outflow tract (52). Together, the presence of these motifs and their linked TFs in our potential CHD-enhancers highlights their possible role in early heart development and maturation.

#### **Table 1: A list of significantly enriched Transcription Factor Binding Sites (TFBSs) identified within CHD-enhancers through motif enrichment analysis.**

The "Motif" column represents the DNA sequence of each binding site; "TF" specifies the transcription factor, and "q-Value" indicates the statistical significance level of the enriched motif.



Motif	TF	q-Value
	Wt1	0.000236
	KLF4	0.00254
	KLF15	0.00277
	TEAD1	0.00397
	ESR2	0.00529
	Plagl1	0.0125
	NKX2-2	0.0288
	GATA4	0.0405

#### 4. Putative cardiac enhancers and CHD-SNPs showed high conservancy across 99 vertebrate species

Although enhancers are known to be resistant to a certain degree of sequence mutations (53), it is noteworthy to highlight that enhancers with pivotal roles in developmental processes exhibit high conservation across vertebrates (54,55). We therefore sought to employ evolutionary conservation analysis of CHD-enhancers and their CHD-SNPs across 99 distantly related vertebrate species (56). We identified 131 conserved enhancers (131/2056, 6.37%) out of total 2,056 putative enhancers, with significantly high mean *phastCons* score  $\geq 0.6$  (55). Among these, 33 (33/2056, 1.60%) revealed ultra-high sequence conservation *phastCons* score  $\geq 0.8$  (57) (**Table S8**). To validate the significance of the evolutionary conservation observed in putative cardiac enhancers, we compared their conservation scores with randomly generated genomic sequences. This comparison allowed us to determine whether the observed conservation in our enhancers is indeed enhancer specific or merely reflective of broader genomic patterns. From this comparison, we obtained a mean conservation score of 0.2143 ( $SD = 0.2243$ ) within the identified set of putative cardiac enhancers. In contrast, conservation analysis of random sequences revealed low mean conservation value 0.08264 ( $SD = 0.1501$ ). Statistically significant differences were obtained between the conservation scores of compared groups with  $p$  value  $< 2.2e^{-16}$  from *Wilcoxon* rank sum test. The higher conservation scores for putative cardiac enhancers in comparison to random genomic elements suggest their vital evolutionary function (**Fig 2D**) and highlight their functional relevance in cardiac development. Furthermore, determining per-nucleotide conservation of CHD-SNP locations revealed 48 conserved variants with *phyloP* score  $\geq 6.0$  contained across 99 vertebrate species (**Table S9**).

To further determine the potential functional impact of CHD-SNPs on their target gene expression, we investigated the presence of regulatory SNPs (rSNPs) with known expression quantitative trait loci (eQTLs obtained from GTEx (58) database) in CHD-enhancers. We found 63 CHD-SNPs with known eQTLs which were distributed across various cardiac tissues, including 16 in the aorta, 9 in the coronary artery, 23 in the heart atrial appendage, and 15 in the left ventricle. These variants were designated as regulatory CHD-SNPs (rCHD-SNPs; **Table S10**). Notably, among rCHD-SNPs, an intronic variant *rs12724121* (chr1:236688982-236688983) was situated within a conserved CHD-enhancer element (chr1:236688907-236689057). This region aligns with DNaseI open chromatin regions from fetal heart tissue and also contained multiple TFBSs, including those specific to cardiac function (**Fig 3**). The presence of *rs12724121* in this evolutionarily conserved context suggests its potential regulatory role in cardiac-related processes. Moreover, the convergence of conservation, enhancer-specific histone modification marks, and TFBS density highlights the intricate regulatory landscape surrounding this particular CHD-SNP.

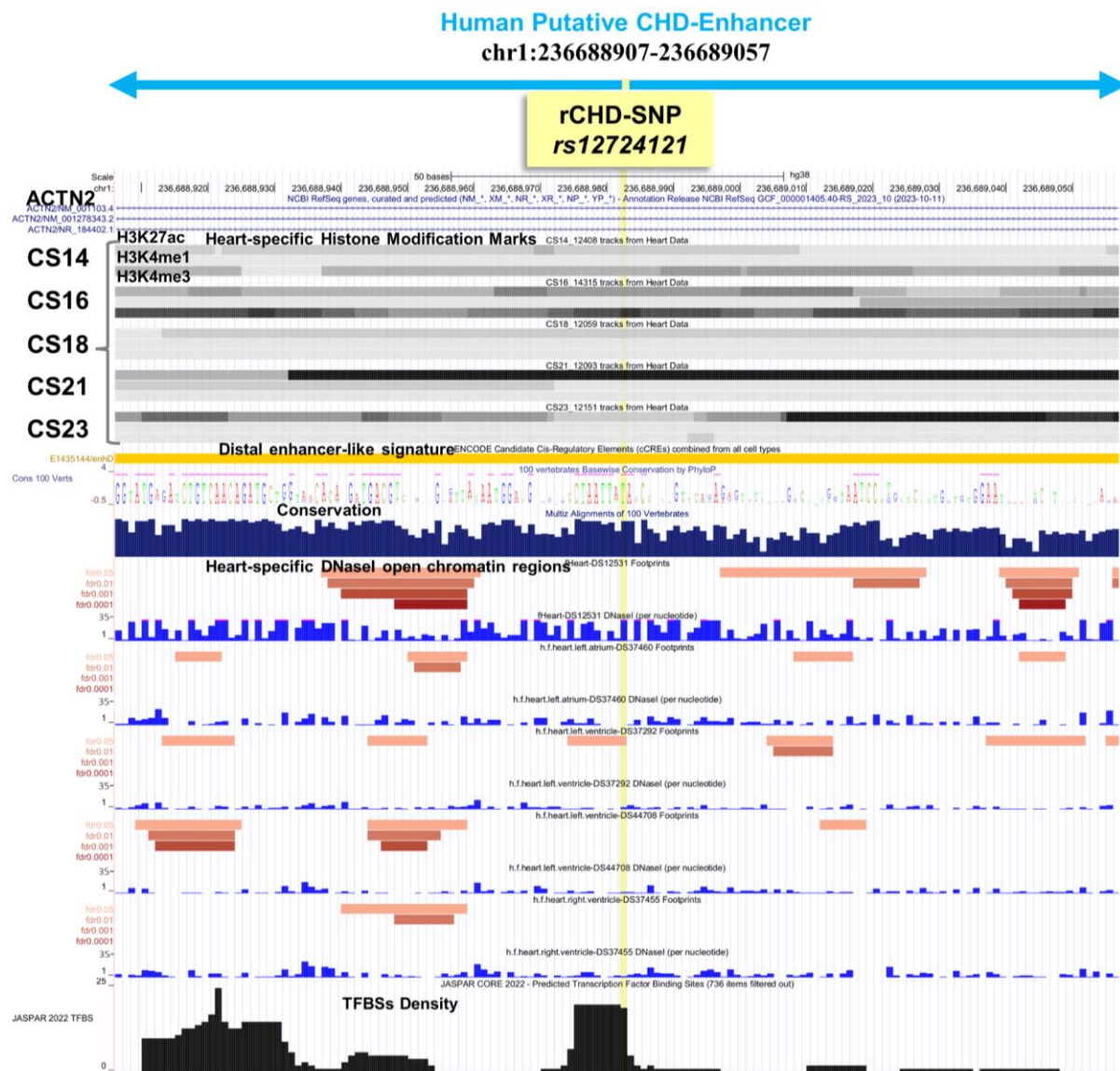


**Fig 3:** A screenshot captured from the UCSC genome browser illustrates a conserved human putative CHD-enhancer. The predicted enhancer resides within the intronic region of the *ACTN2* gene (chr1:236688907-236689057) and encompasses a regulatory CHD-SNP (rCHD-SNP; chr1:236688982-236688983 *rs12724121*, highlighted in 'yellow'). The displayed enhancer region exhibits evolutionary conservation and is covered with heart-specific histone modification marks across 5 Carnegie stages (CS14, CS16, CS18, CS21, and CS23). It features a distal enhancer-like signature from the ENCODE registry of candidate *cis*-Regulatory Elements track. This region is further characterized by heart-specific DNaseI-hypersensitive sites (DNaseI), as obtained from the data by Vierstra *et al.* (81) and integrated as a UCSC track and exhibits overlap with a high density of transcription factor binding sites (TFBSs) from the Jaspasr 2022 core vertebrates TFs database track.

### 5. CHD-SNPs within the coding regions can disrupt the protein-protein binding efficiency

SNPs within protein-coding genes can potentially disrupt protein-protein interactions, leading to abnormal cellular signaling and developmental defects that may contribute to CHD pathogenesis (17,59,60). To examine this, a protein-protein interaction network (PPIN) was

constructed from the set of genes encompassing 11,770 coding CHD-SNPs. PPIN (**Fig S1**) consists of 306 proteins (286 genes from our query and 20 additional genes resulting from GeneMania-Cytoscape module output (61,62)) with 675 edges (connecting physically interacting proteins). The clustering analysis of the PPIN identified 16 functional modules. These clusters ranged in size, with the largest cluster, denoted as cluster 1 (**Fig S2**) encompassing 72 proteins and 304 edges. The smallest cluster consisted of only 3 nodes and 2 edges. Next, to study the impact of SNPs on the binding affinity of the physically interacting proteins, we selected two cardiac sarcomeric proteins from cluster-1 namely, cardiac myosin binding protein-C (*MYBPC3*) and cardiac  $\alpha$ -actin (*ACTC1*) (16) (**Fig 4A, B**). Prior studies revealed a substantial number of individuals with hypertrophic cardiomyopathy (HCM) and dilated cardiomyopathy exhibit alterations in sarcomeric proteins (17,18). Therefore, to analyze the effect of CHD-SNPs on sarcomeric proteins, we obtained an experimentally resolved protein complex for *MYBPC3-ACTC1*(18) from protein data bank (PDB). Subsequently, the structural analysis of this protein complex (using PDBePISA (63)) revealed 15 interface residues and the remaining 331 residues were located on its surface. Changes in binding energy, a measure to assess protein complex stability ( $\Delta\Delta G$ ) was computed for 15 distinct mutations (exonic CHD-SNPs) and assessed their impact on protein binding stability using MutaBind2 (64) (**Table 2**). From this analysis, we found a specific CHD-SNP (*rs770030288*) which is located in C2 domain of *MYBPC3* protein with arginine to histidine substitution at 419 position has deleterious effect, which may impair its interaction with *ACTC1* protein. Notably, the evolutionary analysis of *MYBPC3* protein sequence using ConSurf (65) also detects high conservancy of arginine, highlighting the functional importance of this residue in preserving the conformational stability of the protein (**Fig 4C**). Moreover, upon inducing the R419H mutation, histidine (mutated residue) interacts with only 70 other atoms in vicinity (**Fig 4D (b, d)**) while the non-mutated form arginine interacts with 152 atoms, suggesting structural instability upon mutation (**Fig 4D (a, c)**).







### Table 2: Mutabind analysis of CHD-SNPs impact on Protein-Protein binding affinity.

The columns “Protein 1 chain” and “Protein 2 chain” represents the protein 1 and protein 2 chains in a complex, “Mutated Chain” column represents the mutated protein chain, “Mutation” specifies the mutation, “DDG” quantifies the variation in free energy upon mutation and its impact on protein complex stability. A mutation is classified as deleterious if  $DDG \geq 1.5$  or  $\leq -1.5$  kcal mol<sup>-1</sup>. The column “Interface” indicates if the mutation occurs at the protein-protein interface or not.

Protein 1 chain	Protein 2 chain	Mutated Chain	CHD-SNP	DDG	Interface	Deleterious
A	G	G	<b>R419H</b>	<b>1.64</b>	no	<b>yes</b>
A	G	G	K380R	0.44	yes	no
A	G	G	E451Q	0.03	no	no
A	G	G	G416S	1.35	no	no
A	G	G	E441K	1.23	no	no
A	G	G	F448S	0.29	no	no
A	G	G	A364T	0.41	no	no
A	G	G	A429V	-0.02	no	no
A	G	G	K380N	1.08	yes	no
A	G	G	K380R	0.44	yes	no
A	G	A	N92S	0.3	no	no
A	G	A	G245D	1.27	no	no
A	G	A	I267T	0.6	no	no
A	G	A	F21L	0.44	yes	no
A	G	A	L8M	0.19	no	no

### Discussion

Our study aimed to investigate the contribution of SNPs located in both the noncoding and coding parts of the genome, and potential disruptions caused by them, on the gene regulatory system associated with congenital heart disease (CHD). Using publicly available human genomics data, we developed a computational pipeline to identify a robust set of SNPs associated with CHD. Significantly, a substantial portion of noncoding CHD-SNPs coincided with histone modification marks indicating enhancer activity specific for heart development. These regions, termed CHD-enhancers, were found enriched for important heart-specific transcription factor binding motifs, indicating their regulatory roles. Notably, a subset of identified CHD-enhancers, including the associated CHD-SNPs, exhibited a remarkable degree of conservation among vertebrates, implying their potential functional contribution in heart development. Moreover, in our analysis, a subset of the identified CHD-SNPs was discovered to align with known expression Quantitative Trait Loci (eQTLs). These specific genetic variants, termed regulatory CHD-SNPs (rCHD-SNPs), suggest a functional association with gene expression dysregulation.

From the coding CHD-SNPs, we studied how they might affect the protein-protein interactions in a network by introducing a series of mutations in protein structures. We predicted a highly conserved coding CHD-SNP (p. R419H) in cardiac sarcomeric protein *MYBPC3* which might negatively impact its interaction with another sarcomeric protein, *ACTC1*. A subset of CHD-associated SNPs in the noncoding region did not overlap with any enhancer marks. One possibility is that these SNPs could affect the function of noncoding transcripts. Many noncoding RNA have been implicated in heart development and disease (66,67). While our study focused on the effects of SNPs on enhancer region, those affecting the noncoding RNAs were not within the scope of our analysis. However, there are good examples of other studies

dedicated to this topic. Zhu *et al.* presented a systematic methodology to analyze noncoding RNAs in the context of cardiovascular diseases which led to the identification of a novel ncRNA, *IGBP1P1*, whose depletion has been shown to restore cardiac function in disease (68). Liu *et al.* pinpointed key SNPs associated with Atrial Septal Defect as eQTLs for the lncRNA *STX18-AS1* (69). Another study by Hakansson *et al.* presented a link between SNPs within the 14q32 snoRNA locus and cardiovascular diseases in a substantial population-based investigation (70). As more and more noncoding transcripts are being identified their contribution to the CHD pathogenesis can be better understood.

With the increased capacity of genomics to discover disease-related SNPs, the repository will become increasingly enriched with *de novo* SNPs. Richter and colleagues (71) undertook such efforts, utilizing a machine learning approach to identify *de novo* noncoding variants by comparing whole genome sequences from 749 CHD patients with their parents and 1,611 child-parent healthy trios. Additionally, another study by Rummel *et al.* utilized massively parallel variant annotation to identify functionally important noncoding variants associated with Schizophrenia (72). These examples are expected to further expand our knowledge on the contribution of *de novo* mutations in various diseases and offer valuable insights into their mechanism. In conclusion, our study offers a systematic catalog of genetic variants associated with CHD. We explored their potential implications in impairing enhancer regulatory functions and disrupting protein-protein interactions. Our findings illuminate the intricate interplay between noncoding and coding SNPs, shedding light on a plausible mechanism contributing to CHD pathology.

## Materials and Methods

### 1. Data collection and computational framework design

A computational pipeline (**Fig 1A**) was designed to identify genetic variants associated with congenital heart disease (CHD) in both coding and noncoding regions of the genome. Data was collected from the GWAS-catalog (19) and ClinVar (20,21) database, capturing a broad range of genetic variations and their corresponding phenotypes, including both benign and pathogenic variants. From these datasets, CHD-specific SNPs were isolated based on 56 CHD-associated traits derived from several public databases and literature including “congenital heart disease”, “cardiac septal defects”, “heart structural deformities”, “non-syndromic CHD”, “CHD subtypes” (22–25) (**Table S1**). Next, ANNOVAR (26) was employed to classify these CHD-SNPs as either coding or noncoding, followed by specific computational analysis steps. For noncoding CHD-SNPs, genomic coordinates were expanded by 75bp both upstream and downstream of the SNP location, creating two subsets: one from the GWAS-catalog and another from ClinVar, each featuring a 150bp segment centered on the CHD-SNP (**Fig 1(a)**). These subsets then served in identifying putative cardiac enhancers (detailed in section 2 of methods). To study the impact of coding CHD-SNPs and determine the influence of missense mutations on the stability of protein complexes (detailed in sections 3 and 4 of methods), we constructed a protein-protein interaction network (PPIN) by incorporating genes containing CHD-SNPs in their exons (**Fig 1(b)**).

### 2. Identification of putative cardiac enhancers harbouring CHD-SNPs and their downstream analysis

Within extended genomic segments of 150bp, noncoding CHD-SNPs were probed for the presence of histone modification hallmarks indicative of enhancer activity, namely, H3K27ac, H3K4me1, and H3K4me3 (27–30). Notably, while H3K4me3 is predominantly linked with

promoters, it can occasionally mark enhancers (32,33). For this analysis, epigenomic data from human heart organogenesis were obtained from Cotney's lab ([https://cotneylab.cam.uchc.edu/~jcotney/HEART\\_HUB/hg38/primary/](https://cotneylab.cam.uchc.edu/~jcotney/HEART_HUB/hg38/primary/)) (34). Intersections of these three histone modifications across nine Carnegie stages (CS13, CS14, CS16-21, CS23) with 150bp elements were computed. Subsequently, intersections with threshold of pvalSignal score  $\geq 9.0$  were retained. This step resulted in two sets of putative cardiac enhancers: one from the GWAS-catalog and the other derived from ClinVar database. Both sets were merged to a final unified set of putative cardiac enhancers which were further categorized based on their stage-wise developmental activity, including *early* (exhibiting high-pvalSignal in CS13, CS14 and CS16 for a given element of 150bp), *intermediate* (high-pvalSignal in CS17, CS18 and CS19 for a given element of 150bp), *late* (high-pvalSignal in CS20, CS21 and CS23 for a given element of 150bp) and *constitutively-active* (high-pvalSignal present in all stages for a given element of 150bp) elements. Additionally, pvalSignal was examined for stage combinations, encompassing early-intermediate, early-late, and intermediate-late. Following this, we investigated the presence of regulatory SNPs (rSNPs) within CHD-enhancers by utilizing cardiac eQTL data for Aorta, Coronary Artery, Heart Atrial Appendage, and Heart Left Ventricle from the GTEx database (58). Intersections between SNP locations in CHD-enhancers and eQTL SNP locations were performed and unique matches were retained.

In parallel, motif enrichment analysis was performed on the finalized set of putative cardiac enhancers using FIMO-MEME tool (73,74), with human genome as background. Transcription factor binding profiles were obtained from JASPAR Core database 2022 (75) (PWMs for vertebrates) to compute motif enrichments within enhancer sequences. The identified set of enriched motifs were filtered using threshold of q-value  $\leq 0.05$ . Further, to determine evolutionary significance of identified enhancers, phastCons (55) conservation scores were computed from multiple sequence alignment across 99 vertebrate species downloaded from the UCSC genome browser (56). Average conservation signal within enhancer regions were computed using *bigWigAverageOverBed* (UCSC tools). Next, to determine the robustness of evolutionary conservation detected in CHD-enhancer elements, their conservation scores were compared to randomly generated noncoding genomic sequences. In this process, a set of 10,000 random sequences of 150bp were generated from noncoding human genome and their average conservation signal (*phastCons*) was computed across 99 vertebrate species. Mean conservation scores were compared between putative enhancer and random genomic sequences and statistical significance was computed using *wilcoxon* rank sum test. Further, per-base conservation for CHD-SNPs locations was also determined by calculating *phyloP* (57) conservation scores across 99 vertebrate species. As validation, CHD-enhancer coordinates were cross-referenced with known enhancers from human enhancer disease database (35).

### 3. Protein-Protein interaction network construction from coding CHD-SNPs and protein sequence analysis

To analyze a set of coding CHD-SNPs, PPIN was constructed using GeneMania (61), a plugin within the Cytoscape tool (62). In this network, 'nodes' represented genes containing exonic CHD-SNPs, and the 'edges' illustrated the interactions between physically interacting proteins. Subsequently, clusters within the PPIN were identified based on markov cluster algorithm (76) (MCL; **Fig S2**) from *clusterMaker* plugin (77). To discern functionally significant regions within protein sequences, protein domain analysis was conducted using the Simple Modular Architecture Research Tool (78) (SMART) together with evolutionary conservation analysis using conSurf tool (65). Additionally, for the detection of domains responsible for establishing

protein-protein interactions IntAct molecular interaction database was utilized (<https://www.ebi.ac.uk/intact/home>).

#### 4. Coding CHD-SNPs and their impact on protein-protein interactions

The impact of missense mutations (nonsynonymous coding CHD-SNPs) on protein-protein complex stability (59,60) was evaluated by obtaining a three-dimensional structure of a protein-protein complex from the protein data bank (79). Single mutations were introduced within interacting monomers of the complex using structure editing (rotamers) tool of Chimera (<http://www.cgl.ucsf.edu/chimera/>) (80). Further, change in binding free energy ( $\Delta\Delta G_{bind}$ ) was computed using MutaBind2 (64) for each of the mutated complex, providing a quantitative measure of the mutational impact on protein-protein interaction stability.

$$\Delta\Delta G_{bind} = \Delta G_{bind}^{mut} - \Delta G_{bind}^{WT} \quad (1) \quad (60)$$

Binding energy  $\Delta G_{bind}$  is computed by taking the difference between free energies of bound proteins (AB) and protein monomers in unbound state (A and B):

$$\Delta G_{bind} = \Delta G^{AB} - \Delta G^A - \Delta G^B \quad (2) \quad (60)$$

#### Acknowledgements

This work was supported by the Polish National Science Center (NCN) OPUS grant 2018/29/B/NZ2/01010 and 2022/47/B/NZ2/02926. We thank all the members of ZDG lab for fruitful discussions. We would like to thank M. Pawlak for initial support in the project.

#### Supplementary Information

The supplementary information includes Excel files containing supplementary tables and a document with supplementary figures.

#### Data Availability Statement

The source code and data used to produce the results and analyses presented in this manuscript are available at <https://github.com/rshikha95/CHD-SNPs.git>.

#### Conflict of Interest

We declare no conflicting interests.

#### References

1. van der Linde D, Konings EEM, Slager MA, Witsenburg M, Helbing WA, Takkenberg JJM, et al. Birth Prevalence of Congenital Heart Disease Worldwide. *Journal of the American College of Cardiology*. 2011 Nov;58(21):2241–7.
2. Bernier PL, Stefanescu A, Samoukovic G, Tchervenkov CI. The Challenge of Congenital Heart Disease Worldwide: Epidemiologic and Demographic Facts. *Seminars in Thoracic and Cardiovascular Surgery: Pediatric Cardiac Surgery Annual*. 2010 Jan;13(1):26–34.
3. Hoffman JIE. The global burden of congenital heart disease : review article. *CVJA*. 2013 Jun 21;24(4):141–5.

4. Hoffman JIE, Kaplan S. The incidence of congenital heart disease. *Journal of the American College of Cardiology*. 2002 Jun;39(12):1890–900.
5. Walsh R, Thomson KL, Ware JS, Funke BH, Woodley J, McGuire KJ, et al. Reassessment of Mendelian gene pathogenicity using 7,855 cardiomyopathy cases and 60,706 reference samples. *Genetics in Medicine*. 2017 Feb;19(2):192–203.
6. Pugh TJ, Kelly MA, Gowrisankar S, Hynes E, Seidman MA, Baxter SM, et al. The landscape of genetic variation in dilated cardiomyopathy as surveyed by clinical DNA sequencing. *Genetics in Medicine*. 2014 Aug;16(8):601–8.
7. Yang L, Liu X, Chen Y, Shen B. An update on the CHDGKB for the systematic understanding of risk factors associated with non-syndromic congenital heart disease. *Computational and Structural Biotechnology Journal*. 2021;19:5741–51.
8. Watanabe K, Stringer S, Frei O, Umićević Mirkov M, De Leeuw C, Polderman TJC, et al. A global overview of pleiotropy and genetic architecture in complex traits. *Nat Genet*. 2019 Sep;51(9):1339–48.
9. Villar D, Frost S, Deloukas P, Tinker A. The contribution of non-coding regulatory elements to cardiovascular disease. *Open Biol*. 2020 Jul;10(7):200088.
10. Chahal G, Tyagi S, Ramialison M. Navigating the non-coding genome in heart development and Congenital Heart Disease. *Differentiation*. 2019 May;107:11–23.
11. Soldner F, Stelzer Y, Shivalila CS, Abraham BJ, Latourelle JC, Barrasa MI, et al. Parkinson-associated risk variant in distal enhancer of  $\alpha$ -synuclein modulates target gene expression. *Nature*. 2016 May;533(7601):95–9.
12. Gusev A, Lee SH, Trynka G, Finucane H, Vilhjálmsson BJ, Xu H, et al. Partitioning Heritability of Regulatory and Cell-Type-Specific Variants across 11 Common Diseases. *The American Journal of Human Genetics*. 2014 Nov;95(5):535–52.
13. Corradin O, Scacheri PC. Enhancer variants: evaluating functions in common disease. *Genome Med*. 2014 Oct;6(10):85.
14. Padhy B, Hayat B, Nanda GG, Mohanty PP, Alone DP. Pseudoexfoliation and Alzheimer’s associated CLU risk variant, rs2279590, lies within an enhancer element and regulates CLU, EPHX2 and PTK2B gene expression. *Human Molecular Genetics*. 2017 Nov 15;26(22):4519–29.
15. Rahimov F, Marazita ML, Visel A, Cooper ME, Hitchler MJ, Rubini M, et al. Disruption of an AP-2 $\alpha$  binding site in an IRF6 enhancer is associated with cleft lip. *Nat Genet*. 2008 Nov;40(11):1341–7.
16. Ahmed RE, Tokuyama T, Anzai T, Chanthra N, Uosaki H. Sarcomere maturation: function acquisition, molecular mechanism, and interplay with other organelles. *Phil Trans R Soc B*. 2022 Nov 21;377(1864):20210325.
17. Teng S, Madej T, Panchenko A, Alexov E. Modeling Effects of Human Single Nucleotide Polymorphisms on Protein-Protein Interactions. *Biophysical Journal*. 2009 Mar;96(6):2178–88.
18. Risi CM, Patra M, Belknap B, Harris SP, White HD, Galkin VE. Interaction of the C2 Ig-like Domain of Cardiac Myosin Binding Protein-C with F-actin. *Journal of Molecular Biology*. 2021 Sep;433(19):167178.
19. Buniello A, MacArthur JAL, Cerezo M, Harris LW, Hayhurst J, Malangone C, et al. The NHGRI-EBI GWAS Catalog of published genome-wide association studies, targeted arrays and summary statistics 2019. *Nucleic Acids Research*. 2019 Jan 8;47(D1):D1005–12.
20. Landrum MJ, Kattman BL. ClinVar at five years: Delivering on the promise. *Human Mutation*. 2018 Nov;39(11):1623–30.
21. Landrum MJ, Lee JM, Riley GR, Jang W, Rubinstein WS, Church DM, et al. ClinVar: public archive of relationships among sequence variation and human phenotype. *Nucl Acids Res*. 2014 Jan;42(D1):D980–5.
22. Congenital Heart Disease (CHD) [Internet]. Congenital Heart Disease (CHD). Available from: <https://www.chop.edu/conditions-diseases/congenital-heart-disease>
23. Congenital Heart Defects (CHDs) [Internet]. 2023. Available from: <https://www.cdc.gov/ncbddd/heartdefects/index.html>
24. Blue GM, Kirk EP, Giannoulatou E, Sholler GF, Dunwoodie SL, Harvey RP, et al. Advances in the Genetics of Congenital Heart Disease. *Journal of the American College of Cardiology*. 2017 Feb;69(7):859–70.



25. Van Den Eynde J, Franchi T, Foo YC, Mills B, Ali S, Doulamis IP, et al. The 100 most influential articles in congenital heart disease in 2000–2020: A bibliometric analysis. *International Journal of Cardiology Congenital Heart Disease*. 2021 Aug;4:100156.
26. Wang K, Li M, Hakonarson H. ANNOVAR: functional annotation of genetic variants from high-throughput sequencing data. *Nucleic Acids Research*. 2010 Sep 1;38(16):e164–e164.
27. Heintzman ND, Stuart RK, Hon G, Fu Y, Ching CW, Hawkins RD, et al. Distinct and predictive chromatin signatures of transcriptional promoters and enhancers in the human genome. *Nat Genet*. 2007 Mar;39(3):311–8.
28. Heintzman ND, Hon GC, Hawkins RD, Kheradpour P, Stark A, Harp LF, et al. Histone modifications at human enhancers reflect global cell-type-specific gene expression. *Nature*. 2009 May;459(7243):108–12.
29. Heintzman ND, Ren B. Finding distal regulatory elements in the human genome. *Current Opinion in Genetics & Development*. 2009 Dec;19(6):541–9.
30. Visel A, Blow MJ, Li Z, Zhang T, Akiyama JA, Holt A, et al. ChIP-seq accurately predicts tissue-specific activity of enhancers. *Nature*. 2009 Feb 12;457(7231):854–8.
31. Creighton MP, Cheng AW, Welstead GG, Kooistra T, Carey BW, Steine EJ, et al. Histone H3K27ac separates active from poised enhancers and predicts developmental state. *Proc Natl Acad Sci USA*. 2010 Dec 14;107(50):21931–6.
32. Beacon TH, Delcuve GP, López C, Nardocci G, Kovalchuk I, Van Wijnen AJ, et al. The dynamic broad epigenetic (H3K4me3, H3K27ac) domain as a mark of essential genes. *Clin Epigenet*. 2021 Dec;13(1):138.
33. Chen K, Chen Z, Wu D, Zhang L, Lin X, Su J, et al. Broad H3K4me3 is associated with increased transcription elongation and enhancer activity at tumor-suppressor genes. *Nat Genet*. 2015 Oct;47(10):1149–57.
34. VanOudenhove J, Yankee TN, Wilderman A, Cotney J. Epigenomic and Transcriptomic Dynamics During Human Heart Organogenesis. *Circ Res [Internet]*. 2020 Oct 9 [cited 2023 Dec 18];127(9). Available from: <https://www.ahajournals.org/doi/10.1161/CIRCRESAHA.120.316704>
35. Wang Z, Zhang Q, Zhang W, Lin JR, Cai Y, Mitra J, et al. HEDD: Human Enhancer Disease Database. *Nucleic Acids Research*. 2018 Jan 4;46(D1):D113–20.
36. Spitz F, Furlong EEM. Transcription factors: from enhancer binding to developmental control. *Nat Rev Genet*. 2012 Sep;13(9):613–26.
37. Grossman SR, Zhang X, Wang L, Engreitz J, Melnikov A, Rogov P, et al. Systematic dissection of genomic features determining transcription factor binding and enhancer function. *Proc Natl Acad Sci USA [Internet]*. 2017 Feb 14 [cited 2023 Dec 18];114(7). Available from: <https://pnas.org/doi/full/10.1073/pnas.1621150114>
38. Harismendy O, Notani D, Song X, Rahim NG, Tanasa B, Heintzman N, et al. 9p21 DNA variants associated with coronary artery disease impair interferon- $\gamma$  signalling response. *Nature*. 2011 Feb;470(7333):264–8.
39. Duim SN, Kurakula K, Goumans MJ, Kruithof BPT. Cardiac endothelial cells express Wilms' tumor-1. *Journal of Molecular and Cellular Cardiology*. 2015 Apr;81:127–35.
40. Pikkarainen S. GATA transcription factors in the developing and adult heart. *Cardiovascular Research*. 2004 Aug;63(2):196–207.
41. Santoyo-Suarez MG, Mares-Montemayor JD, Padilla-Rivas GR, Delgado-Gallegos JL, Quiroz-Reyes AG, Roacho-Perez JA, et al. The Involvement of Krüppel-like Factors in Cardiovascular Diseases. *Life*. 2023 Feb 2;13(2):420.
42. Kwon IS, Wang W, Xu S, Jin ZG. Histone deacetylase 5 interacts with Krüppel-like factor 2 and inhibits its transcriptional activity in endothelium. *Cardiovascular Research*. 2014 Oct 1;104(1):127–37.
43. Vermot J, Forouhar AS, Liebling M, Wu D, Plummer D, Gharib M, et al. Reversing Blood Flows Act through *klf2a* to Ensure Normal Valvulogenesis in the Developing Heart. Hamada H, editor. *PLoS Biol*. 2009 Nov 17;7(11):e1000246.
44. Liao X, Haldar SM, Lu Y, Jeyaraj D, Paruchuri K, Nahori M, et al. Krüppel-like factor 4 regulates pressure-induced cardiac hypertrophy. *Journal of Molecular and Cellular Cardiology*. 2010 Aug;49(2):334–8.

45. Hamik A, Lin Z, Kumar A, Balcells M, Sinha S, Katz J, et al. Kruppel-like Factor 4 Regulates Endothelial Inflammation. *Journal of Biological Chemistry*. 2007 May;282(18):13769–79.
46. Fisch S, Gray S, Heymans S, Haldar SM, Wang B, Pfister O, et al. Kruppel-like factor 15 is a regulator of cardiomyocyte hypertrophy. *Proc Natl Acad Sci USA*. 2007 Apr 24;104(17):7074–9.
47. Liu Z, Huang S. Upregulation of SPI1 during myocardial infarction aggravates cardiac tissue injury and disease.
48. Liu R, Lee J, Kim BS, Wang Q, Buxton SK, Balasubramanyam N, et al. Tead1 is required for maintaining adult cardiomyocyte function, and its loss results in lethal dilated cardiomyopathy. *JCI Insight*. 2017 Sep 7;2(17):e93343.
49. Luo T, Kim JK. The Role of Estrogen and Estrogen Receptors on Cardiomyocytes: An Overview. *Canadian Journal of Cardiology*. 2016 Aug;32(8):1017–25.
50. Henry S, Kokity L, Purity MK. Polycomb protein RYBP activates transcription factor *Plagl1* during *in vitro* cardiac differentiation of mouse embryonic stem cells. *Open Biol*. 2023 Feb;13(2):220305.
51. Xuan C, Wang BB, Gao G, Bai XY, Yang Q, Liu XC, et al. A Novel Variation of *PLAGL1* in Chinese Patients with Isolated Ventricular Septal Defect. *Genetic Testing and Molecular Biomarkers*. 2012 Aug;16(8):984–7.
52. Gandhi S, Ezin M, Bronner ME. Reprogramming Axial Level Identity to Rescue Neural-Crest-Related Congenital Heart Defects. *Developmental Cell*. 2020 May;53(3):300–315.e4.
53. Snetkova V, Ypsilanti AR, Akiyama JA, Mannion BJ, Plajzer-Frick I, Novak CS, et al. Ultraconserved enhancer function does not require perfect sequence conservation. *Nat Genet*. 2021 Apr;53(4):521–8.
54. Woolfe A, Goodson M, Goode DK, Snell P, McEwen GK, Vavouri T, et al. Highly Conserved Non-Coding Sequences Are Associated with Vertebrate Development. Sean Eddy, editor. *PLoS Biol*. 2004 Nov 11;3(1):e7.
55. Siepel A, Bejerano G, Pedersen JS, Hinrichs AS, Hou M, Rosenbloom K, et al. Evolutionarily conserved elements in vertebrate, insect, worm, and yeast genomes. *Genome Res*. 2005 Aug;15(8):1034–50.
56. Kent WJ, Sugnet CW, Furey TS, Roskin KM, Pringle TH, Zahler AM, et al. The Human Genome Browser at UCSC.
57. Pollard KS, Hubisz MJ, Rosenbloom KR, Siepel A. Detection of nonneutral substitution rates on mammalian phylogenies. *Genome Res*. 2010 Jan;20(1):110–21.
58. The GTEx Consortium, Ardlie KG, Deluca DS, Segrè AV, Sullivan TJ, Young TR, et al. The Genotype-Tissue Expression (GTEx) pilot analysis: Multitissue gene regulation in humans. *Science*. 2015 May 8;348(6235):648–60.
59. Yates CM, Sternberg MJE. The Effects of Non-Synonymous Single Nucleotide Polymorphisms (nsSNPs) on Protein–Protein Interactions. *Journal of Molecular Biology*. 2013 Nov;425(21):3949–63.
60. Li M, Goncarenco A, Panchenko AR. Annotating Mutational Effects on Proteins and Protein Interactions: Designing Novel and Revisiting Existing Protocols. In: Comai L, Katz JE, Mallick P, editors. *Proteomics [Internet]*. New York, NY: Springer New York; 2017 [cited 2023 Dec 17]. p. 235–60. (Methods in Molecular Biology; vol. 1550). Available from: [http://link.springer.com/10.1007/978-1-4939-6747-6\\_17](http://link.springer.com/10.1007/978-1-4939-6747-6_17)
61. Montojo J, Zuberi K, Rodriguez H, Kazi F, Wright G, Donaldson SL, et al. GeneMANIA Cytoscape plugin: fast gene function predictions on the desktop. *Bioinformatics*. 2010 Nov 15;26(22):2927–8.
62. Shannon P, Markiel A, Ozier O, Baliga NS, Wang JT, Ramage D, et al. Cytoscape: A Software Environment for Integrated Models of Biomolecular Interaction Networks. *Genome Res*. 2003 Nov;13(11):2498–504.
63. Krissinel E, Henrick K. Inference of Macromolecular Assemblies from Crystalline State. *Journal of Molecular Biology*. 2007 Sep;372(3):774–97.
64. Zhang N, Chen Y, Lu H, Zhao F, Alvarez RV, Goncarenco A, et al. MutaBind2: Predicting the Impacts of Single and Multiple Mutations on Protein-Protein Interactions. *iScience*. 2020 Mar;23(3):100939.
65. Ashkenazy H, Abadi S, Martz E, Chay O, Mayrose I, Pupko T, et al. ConSurf 2016: an improved

- methodology to estimate and visualize evolutionary conservation in macromolecules. *Nucleic Acids Res.* 2016 Jul 8;44(W1):W344–50.
66. Dueñas A, Expósito A, Aranega A, Franco D. The Role of Non-Coding RNA in Congenital Heart Diseases. *JCDD.* 2019 Apr 1;6(2):15.
  67. Poller W, Dimmeler S, Heymans S, Zeller T, Haas J, Karakas M, et al. Non-coding RNAs in cardiovascular diseases: diagnostic and therapeutic perspectives. *European Heart Journal.* 2018 Aug 1;39(29):2704–16.
  68. Zhu C, Baumgarten N, Wu M, Wang Y, Das AP, Kaur J, et al. CVD-associated SNPs with regulatory potential reveal novel non-coding disease genes. *Hum Genomics.* 2023 Jul 25;17(1):69.
  69. Liu Y, Choy M kit, Abraham S, Tenin G, Black GC, Keavney BD. Atrial Septal Defect (ASD) associated long non-coding RNA STX18-AS1 maintains time-course of in vitro cardiomyocyte differentiation. *Genes & Diseases.* 2023 Jul;10(4):1150–3.
  70. Håkansson KEJ, Goossens EAC, Trompet S, Van Ingen E, De Vries MR, Van Der Kwast RVCT, et al. Genetic associations and regulation of expression indicate an independent role for 14q32 snoRNAs in human cardiovascular disease. *Cardiovascular Research.* 2019 Aug 1;115(10):1519–32.
  71. Richter F, Morton SU, Kim SW, Kitaygorodsky A, Wasson LK, Chen KM, et al. Genomic analyses implicate noncoding de novo variants in congenital heart disease. *Nat Genet.* 2020 Aug;52(8):769–77.
  72. Rummel CK, Gagliardi M, Ahmad R, Herholt A, Jimenez-Barron L, Murek V, et al. Massively parallel functional dissection of schizophrenia-associated noncoding genetic variants. *Cell.* 2023 Nov;186(23):5165-5182.e33.
  73. Bailey TL, Boden M, Buske FA, Frith M, Grant CE, Clementi L, et al. MEME SUITE: tools for motif discovery and searching. *Nucleic Acids Research.* 2009 Jul 1;37(Web Server):W202–8.
  74. Grant CE, Bailey TL, Noble WS. FIMO: scanning for occurrences of a given motif. *Bioinformatics.* 2011 Apr 1;27(7):1017–8.
  75. Castro-Mondragon JA, Riudavets-Puig R, Rauluseviciute I, Berhanu Lemma R, Turchi L, Blanc-Mathieu R, et al. JASPAR 2022: the 9th release of the open-access database of transcription factor binding profiles. *Nucleic Acids Research.* 2022 Jan 7;50(D1):D165–73.
  76. Enright AJ. An efficient algorithm for large-scale detection of protein families. *Nucleic Acids Research.* 2002 Apr 1;30(7):1575–84.
  77. Morris JH, Apeltsin L, Newman AM, Baumbach J, Wittkop T, Su G, et al. clusterMaker: a multi-algorithm clustering plugin for Cytoscape. *BMC Bioinformatics.* 2011 Dec;12(1):436.
  78. Schultz J, Milpetz F, Bork P, Ponting CP. SMART, a simple modular architecture research tool: Identification of signaling domains. *Proc Natl Acad Sci USA.* 1998 May 26;95(11):5857–64.
  79. Berman HM. The Protein Data Bank. *Nucleic Acids Research.* 2000 Jan 1;28(1):235–42.
  80. Pettersen EF, Goddard TD, Huang CC, Couch GS, Greenblatt DM, Meng EC, et al. UCSF Chimera—A visualization system for exploratory research and analysis. *J Comput Chem.* 2004 Oct;25(13):1605–12.
  81. Vierstra J, Lazar J, Sandstrom R, Halow J, Lee K, Bates D, et al. Global reference mapping of human transcription factor footprints. *Nature.* 2020 Jul 30;583(7818):729–36.